Ecotoxicology and Environmental Safety 289 (2025) 117428

Contents lists available at ScienceDirect

Ecotoxicology and Environmental Safety

journal homepage: www.elsevier.com/locate/ecoenv

Microplastic analysis in soils: A comparative assessment

Stoyana Peneva [a,d,1], Quynh Nhu Phan Le [b,1], Davi R. Munhoz [c,1], Olivia Wrigley [d], Flora Wille [e], Heidi Doose [f,g], Crispin Halsall [b], Paula Harkes [c], Michael Sander [e], Melanie Braun [d,*,1], Wulf Amelung [d,h]

[a] Wessling GmbH, AM Umweltpark 1, Bochum 44793, Germany
[b] Lancaster Environment Centre, Lancaster University, Lancaster LA1 4YQ, UK
[c] Soil Physics and Land Management Group, Wageningen University & Research, P.O. Box 47, Wageningen 6700 AA, the Netherlands
[d] Institute of Crop Science and Resource Conservation (INRES), Soil Science and Soil Ecology, University of Bonn, Nussallee 13, Bonn 53115, Germany
[e] Insitute of Biogeochemistry and Pollutant Dynamics, ETH Zurich, Zurich 8092, Switzerland
[f] Co.KG, Feodor-Lynen Straße 23, Hannover 30625, Germany
[g] Wessling Consulting Engineering GmbH & Feodor-Lynen Straß~e 23, Hannover 30625, Germany
[h] Agrosphere Institute (IBG-3), Forschungszentrum Jülich GmbH, Wilhelm-Johnen-Str, Jülich 52425, Germany

ARTICLE INFO

Keywords:
Spectroscopy
Soil pollution
Conventional synthetic and biodegradable polymers

ABSTRACT

Microplastic (MiP) contamination poses environmental risks, but harmonizing data from different quantification methods and sample matrices remains challenging. We compared analytical protocols for MiP quantification in soil, consisting of Digital, Fluorescence, Fourier-transform infrared (FTIR), and Raman Microscopy as well as quantitative Pyrolysis-Gas Chromatography-Mass Spectroscopy (Py-GC-MS) and 1-proton nuclear magnetic resonance (^{1}H NMR) spectroscopy as detection techniques. Each technique was coupled with a specific extraction procedure and evaluated for three soils with different textures and organic carbon contents, amended with eight types of large MiPs (0.5–1 mm) – high- and low-density polyethylene (HDPE and LDPE), polypropylene (PP), polystyrene (PS), polyamide (PA), polyethylene terephthalate (PET), polyvinyl chloride (PVC), and a biodegradable mulch film product composed of polybutylene adipate-co-terephthalate/ polylactic acid (PBAT/ PLA). In addition, we included two types of small MiPs (20–250 μm) composed of either LDPE or PBAT/ PLA in the tests. The results showed that protocols for Digital, Fluorescence, and ATR-FTIR microscopy recovered 74–98 % of the large MiPs, with fluorescence yielding the highest recoveries. Raman spectroscopy was most sensitive to soil organic matter residues, requiring more sophisticated sample pretreatment. Fluorescence staining with subsequent Fluorescence microscopy detection effectively recovered most small-sized LDPE-MiP but missed 56–93 % of small PBAT/ PLA particles. For the latter, reliable quantification was achieved only using Soxhlet extraction combined with ^{1}H NMR spectroscopic quantification. Pyrolysis-GC-MS showed intermediate results, displaying low sensitivity to plastic type and lower recoveries as soil clay content increased. We conclude that different methods have different sensitivities for different MiP materials in different soils, i.e. comparisons of MiP loads and threshold settings for MiP loads across methodologies require careful consideration. Yet, our data indicate that adding stained large MiP as an internal standard could enhance extraction control, while Soxhlet-extraction with subsequent ^{1}H NMR analysis is most powerful for controlling future thresholds of small MiP from biodegradable materials.

1. Introduction

Since the first fully synthetic polymer material was discovered in the early 20th century, plastic materials have found widespread use due to their outstanding chemical and physical properties such as their inertness, lightweight, and flexible usability, as well as their fast production at low cost. In the meantime, consumption of plastics has quadrupled over the past 30 years, resulting in a total global plastic production of 400.3 Mio t in 2022 (OECD, 2022; PlasticsEurope, 2023). Because of mismanaged waste, a significant fraction of plastics ends up

---

* Corresponding author.
E-mail address: melanie.braun@uni-bonn.de (M. Braun).
[1] *Shared first authorship*

https://doi.org/10.1016/j.ecoenv.2024.117428
Received 7 May 2024; Received in revised form 21 November 2024; Accepted 26 November 2024

in the environment (OECD, 2022). Consequently, macroplastics (MaPs, $>$ 2.5 cm), mesoplastics (5 mm - 2.5 cm), and microplastics (MiPs, 1 µm – 5 mm) have been found in both aquatic and terrestrial ecosystems (Lebreton et al., 2017; Sajjad et al., 2022). Yet, reliable extraction and accurate quantification in various environments, especially in soils, remains challenging (Astner et al., 2023; Wang et al., 2023). Current reports point to highly variable MiP loads, which could reflect different plastic exposure and input pathways (e.g., plastic mulching, application of compost or sewage sludge) as well as more diffuse sources (such as flooding of rivers, lakes, and seawater, littering or atmospheric deposition; Büks and Kaupenjohann, 2020; Zhou et al., 2020; Braun et al., 2023). However, variations in the reported MiP concentrations in soil could also reflect differences in analytical protocols used for MiP isolation and detection, with different sensitivities to plastic types, sizes and masses, and limits of detection (Bläsing and Amelung, 2018; Büks and Kaupenjohann, 2020; Primpke et al., 2020a,2020b; Wrigley et al., 2024).

Most extraction methods for analyzing MiPs in soil contain two removal steps, one for the mineral phase and one for soil organic matter (SOM; Möller et al., 2020). The removal of the mineral phase is mostly accomplished by density separation: a salt solution with a specific density higher than the one of the plastic is used to separate minerals from plastics which float on the solution surface and can be collected (Coppock et al., 2017; Ribeiro-Claro et al., 2017). Sodium chloride (NaCl) is the preferred salt by most scientists, due to its low price and lack of toxicity (Han et al., 2019). However, using NaCl achieves a maximum density of only 1.2 g mL^{-1}, insufficient for extracting high-density plastics like polyvinyl chloride (PVC) or polyethylene terephthalate (PET), both of which have a density of appr. 1.37 g mL^{-1}. Hence, other solutions, such as zinc chloride ($ZnCl_2$), adjustable to a density of up to 2.1 g mL^{-1}, have been recommended for isolating plastic particles with higher densities (Mintenig et al., 2016; Löder et al., 2017; El Hayany et al., 2020). However, caution is required when working and disposing of $ZnCl_2$ or sodium iodide (NaI), which are suitable for extracting of high-density plastics, but are considered hazardous (Perez et al., 2022). Besides, $ZnCl_2$ is a rather strong Lewis acid, thus potentially altering biodegradable plastics upon use.

The extracted plastic fraction, however, also contains SOM, which may interfere with MiP identification. Therefore, several studies use an acid, alkaline, enzymatic, or oxidative pretreatment for SOM removal, e. g., using oxidative agents like hydrogen peroxide (H_2O_2) or Fenton's reagent (H_2O_2 with iron(II) sulfate, $FeSO_4$ as a catalyst; Zhou et al., 2020; Junhao et al., 2021). While methods such as Fenton's reaction or strong or alkaline acidic digestion pose the risk of degrading some polymer types (Nuelle et al., 2014; Radford et al., 2021), enzymes can be considered as more gentle reagents (Löder et al., 2017; He et al., 2018; Zhang et al., 2018), and may not completely eliminate SOM. These mineral phase and SOM removal steps have advantages and limitations, requiring careful consideration in protocols for MiP analysis.

The extent to which SOM needs to be removed also depends on the microscopic and spectroscopic technology subsequently used for MiP detection. While larger particles (>0.5 mm) can be identified by eye and removed by hand, for smaller particles, optical microscopy can be used (Mani et al., 2019; Möller et al., 2021; Perez et al., 2022; Braun et al., 2023). Fluorescent staining, using Nile red (NR) as an example fluorophore, combined with automated detection of the stained particles, accelerates MiP detection (Shim et al., 2016). However, there is a risk of false positive results due to the co-staining of SOM with NR, and not all plastics uniformly interact with fluorophores. Moreover, this approach, akin to digital microscopy, cannot differentiate between plastic types (Sturm et al., 2021). For the identification of plastics, techniques like Fourier-transform infrared (FTIR) (Primpke et al., 2020a,2020b) or Raman spectroscopy (Ribeiro-Claro et al., 2017) have been recommended. When operating as an Imaging spectrometer, µ-FTIR can be used for particles of sizes down to 20 µm (Primpke et al., 2018), whereas µ-Raman possesses a better spatial resolution down to 1 µm (Imhof et al., 2012), but also needs exhaustive sample clean-up to prevent SOM auto-fluorescence from distorting the Raman-signal (Löder et al., 2015; Anger et al., 2018). Additionally, the high-resolution mode and accuracy in particle counting makes these techniques very time-consuming (Araujo et al., 2018); sometimes only 1–2 samples can be processed per day. Also, the techniques have specific analytical window for MiP sizes, leading to method inherent challenges particle counting. Yet, a systematic study evaluating the potential of these techniques together for known MiP contaminations in different soils, is still lacking.

In contrast to the above-mentioned particle-based techniques, there are also methods that quantify absolute MiP concentrations without determining MiP sizes. Thermo-extraction desorption (TED-) Gas Chromatography–Mass Spectroscopy (GC-MS) and Pyrolysis (Pyr-) GC-MS have been proposed for this purpose (Dümichen et al., 2017; Kittner et al., 2023). The limit of detection (LOD) for TED- as well as Pyr-GC-MS, depends on several factors, including the MiP type, the applied method for sample preparation, the analytical instrument used, and the expertise of the analyst (El Hayany et al., 2020; Ivleva et al., 2021). Comparing the particle-based and total mass of microplastics (MiP) remains challenging (Caputo et al., 2021). Primpke et al. (2020a), (2020b) explored the detection and identification of microplastics in wastewater, water, and marine sediments using FTIR and Py-GC-MS. While both techniques showed similar trends overall, FTIR often indicated higher concentrations of specific polymer types like PMMA/PUR, whereas Py-GC-MS detected higher shares of PE and PVC. Also, the calculated masses were primarily driven by particles larger than 100 µm. That led to an overestimation of mass, especially for PP, where a few large-sized particles could significantly inflate the calculated masses. Furthermore, TED- and Pyr-GC-MS are typically conducted on extracted materials due to the specificity of the analysis and the potential overlap of pyrolyzed products from plastic with organic compounds and minerals in uncleaned soil samples.

The presence of SOM and contaminants from other soil components can additionally hinder MiP quantification (Primpke et al., 2020a, 2020b). One approach to address this challenge involves dissolving MiPs in solvents before, e.g., Pyr-GC-MS and ^{1}H NMR analyses. Here the solubility of the polymers in the chosen solvent and the heterogeneous nature of the soil matrix has to be considered (Nelson et al., 2019; Steinmetz et al., 2020). Using only one solvent, the application of this method will be limited to polymer types that dissolve in the chosen solvent. Nonetheless, the varying solubility of polymers can allow for the separation and individual analysis of different polymer types. Such logic is also used in a method to quantify polymers using ^{1}H NMR. Recently, ^{1}H NMR has gained attraction for monitoring PBAT/ PLA biodegradation in soils, given its precision and low LOD/ limit of quantification (LOQ) values (1.3 and 4.4 µg mL^{-1} respectively for PBAT in deuterated chloroform ($CDCl_3$; Nelson et al., 2019). Hence, this study tested this method against other potential mass-based (e.g., Py-GC-MS) and particle-based methods for PBAT/ PLA quantification, such as µ-Raman and µ-FTIR. Since these standard analytical techniques are not yet routinely used for biodegradable plastics, we aimed to assess them alongside the established protocol based on solvent extraction and ^{1}H NMR.

In summary, several extraction protocols with subsequent detection techniques for MiPs in soil are available, with their unique strengths and limitations. However, a comparative analysis is missing, which hinders a direct comparison of results from different studies. Hence, our goal was to evaluate the efficiency of commonly used methods to recover MiP particles from soils by adding these particles to different soils in known amounts and particle numbers. We focused on two MiP size ranges: visible pieces in the size range of 500–1000 µm, which provide robust quality control as they are easy to spike and identify, and small MiPs in the size range of ~100 µm diameter, not clearly visible by the naked eye as individual particles. In addition, we selected different polymer types (biodegradable versus non-biodegradable, low-density versus high-density plastics), and performed our analyses with different soil types (sandy, loamy, and clayey mineral soils). The application of all common methods for plastic analyses to the same samples set allows us to provide clearer insights into possible bias of common plastic detection methods towards material origins and soil interferences.

2. Methods and materials

2.1. Soils used for spike-recovery experiments

To assess the potential effects of texture and soil organic carbon content on the extraction of MiPs, we chose three mineral soils with different textures: we used sandy and clayey soils (Cambisol and Stagnosol, respectively) from sampling campaigns near Bonn, Germany, and supplemented it with certified loamy topsoil to allow standardized comparisons in future studies (LUFA soil SP 2.4.; Speyer, Germany). All soils were air-dried and sieved to 2 mm (Table 1). Measured background contaminations were negligibly small for all analytical techniques (Table S1), but for fluorescence microscopy up to 3590 fluorescent particles were detected in loamy soil. However, this count may include false positive results attributed to SOM. Thus, background subtraction is highly important for accurate analyses, especially for the fluorescence technique. (see Results and Discussion section).

2.2. Plastic materials used for recovery experiments

To cover a range of potential polymer types of plastic found as MiP in soil, we used two different MiP size groups, (500–1000 μm and 5–250 μm) and different plastic types as examples for conventional and biodegradable plastics. For larger MiPs (500–1000 μm), we used eight plastic types derived from household products (Table 1 and Figure S1); MiPs were produced using a standard razor blade and ensured to be the desired size with a digital microscope (Zeiss STEMi 305). For small MiPs (5–250 μm), we obtained LDPE microparticles from Goonvean Fibers Ltd (Cullompton, England) and cryo-milled a PBAT/ PLA blend film (BIONOV B, Barbier, France). While LDPE was specified to be 10–150 μm, the PBAT/ PLA was sieved to 100–250 μm. Quality assurance using fluorescence and Raman microscopes, and a particle measuring system (model Syringe, Markus Klotz GmbH) in ethanol suspension revealed actual sizes between 5 and 250 μm for both plastics (Figure S2, Supplementary Materials).

2.3. Spiking of soil samples

To determine the recovery of MiP from the soils by each of the different methodologies, 10 g of each soil (in 3-fold replication) was spiked with large and small MiPs (Table 2): for large MiPs, five particles of each of the eight plastic types were added to the soil, and for small MiPs, 3 mg of each LDPE and PBAT/ PLA was added (Table S2). To minimize particle loss during spiking, MiPs were placed on pre-wetted gelatin sheet, 1 cm×1 cm (one sheet for large particles and two sheets for each LDPE and PBAT/ PLA; Hurley et al., 2018; Zhang et al., 2018), which can be re-dissolved and homogenized in a mixture of soil and water (Möller et al., 2020). Large MiPs were placed onto the gelatin sheet using either non-static tweezers or a needle, while small MiPs were directly weighted on the gelatin sheet. Three gelatin sheets (one with large and two with small MiPs) were added to each soil in a beaker and left overnight, covered with a small amount of water to ensure their dissolution. For the Soxhlet – extraction coupled to ^{1}H NMR analysis, 3 mg of PBAT/ PLA (Table S2) was directly added to the tested soils. For each analytical test, the whole 10 g of spiked soil was processed in replicates.

Table 1
Physicochemical properties of soils used for comparative method assessment.

Texture	Sandy	Loamy (LUFA 2.4.)	Clayey
Organic Carbon, g kg^{-1}	9 ± 2	18 ± 2	59 ± 1
Particle size distribution (mm) (g kg^{-1})			
< 0.002	85 ± 0.5	238 ± 1.5	503 ± 0.5
0.002–0.006	37 ± 7.5	76 ± 6	82 ± 3.7
0.006–0.02	38 ± 2.5	146 ± 10	140 ± 0.3
0.02–0.063	89 ± 6	264 ± 14	141 ± 13.5
0.063–0.2	169 ± 2.5	208 ± 12	58 ± 0.6
0.2–0.63	515 ± 29	55 ± 19	23 ± 2
0.63–2	49 ± 8.5	13 ± 4	1.7±0.4

For each detection technique specific sample preparation is required and was subsequently tested (Fig. 1 and description in Supplementary Materials and Table S3 and S4 for details):

- Method A – Density separation followed by Digital Microscopy analysis (Braun et al., 2021, 2023).
- Method B – Density separation, Fenton's digestion, followed by fluorescence staining and Fluorescence Microscopy (Coppock et al., 2017; Shim et al., 2016).
- Method C – Density separation, Enzymatic, and Fenton's digestion and followed by ATR- and focal plane array (FPA-) μ-FTIR (method C1 and C2), μ-Raman Spectromicroscopy (method C3), and Pyr-GC-MS analysis (method C4; Löder et al., 2017; Mintenig et al., 2017; Primpke et al., 2018; Mbachu et al., 2021).
- Method D - Soxhlet extraction coupled to quantitative ^{1}H NMR spectroscopy (Nelson et al., 2019).

Methods C with excessive SOM removal treatments involved four different detection techniques, equated with C1, C2, C3 and C4, respectively. In line with common reports in the literature, Methods A - Digital Microscope and method C1 – ATR-FTIR were applied for large MiPs only (Perez et al., 2022). In contrast, methods B - Fluorescence Spectroscopy and method C3 - μ-Raman Microscope were used for both small and large MiPs, while methods C2 – FPA - μ-FTIR, C4 – Pyr-GC-MS and D – ^{1}H NMR were used for small MiPs only. It's worth noting that each extraction protocol and subsequent purification protocol is considered to be optimal for matching the respective detection method. For each of the seven analytic techniques included (procedure in Supplementary Materials), one of four extraction methods was selected to match the requirements of the technique. We used $ZnCl_2$ as this salt is the most commonly used salt for extraction when high-density plastics are also included in the analysis (Mintenig et al., 2016; Löder et al., 2017; Prosenc et al., 2021; Way et al., 2022). For the small-sized MiPs, aliquots of samples prepared for μ-FTIR and μ-Raman were used for the Pyr-GC-MS measurements as well. Additionally, to the comparison of spectral libraries and matching indexes we used to evaluate the potential effects of sample pre-treatment on the MiPs, we inspected the large MiP for visual changes (via digital microscope), as these changes might also disturb IR or Raman signals or interfere with the staining efficiency for the Fluorescence Microscope.

Each analytical protocol, except for ^{1}H NMR spectroscopy, begins with a density separation step (Fig. 1). We used a prefiltered $ZnCl_2$ solution with a density of 1.5 g mL^{-1}, which was added in a soil:solution ratio of 1:20 (m/v).

The recovery of small particles for methods C2 - FPA-μ-FTIR and C3 - μ-Raman was calculated as a percentage of the expected number in the aliquot taken. In the case of method B - Fluorescence Microscopy the entire sample was considered when calculating recovery. Specific care to prevent sample contaminations from airborne dust or clothes during setup and spiking was taken in each lab as described in Supplementary Materials.

2.4. Data analysis

Statistical analysis was completed using R (V 4.1.2; (R Core Team, 2018)), with the packages ggplot, tidyverse, and dplyr (Wickham, 2016), car (Fox and Weisberg, 2019), and FSA (Ogle et al., 2023). Data were first tested for normality and homoscedasticity by applying a

Table 2

Characteristics of plastics used for method testing and recovery calculations.

Type	Source	Color	Shape	Size	Density, g/cm^3	Chemical Structure
PP	Milk bottle lids	Transparent	NUF	0.5 – 1 mm	0.91	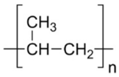
LDPE	Packaging bags	Transparent, with black writing	NUFF	0.5 – 1 mm, 10 – 150 µm powder	0.91–0.93	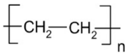
HDPE	Packaging bags	White	NUF	0.5 – 1 mm	0.93–0.97	
PS	Foam - styropor	White	NUF	0.5 – 1 mm	1.02	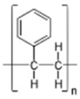
Biodegradable mulch film PBAT/ PLA	Novamont	Black	NUFF	0.5 – 1 mm, 10–250 µm powder	1.23–1.29	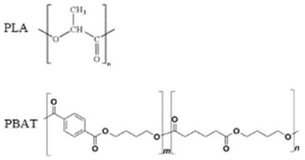
PA - Nylon 6,6	Fishing net	Light brown	UF	0.5 – 1 mm	1.14	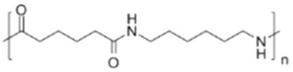
PET	Restaurant boxes	Transparent	UF	0.5 – 1 mm	1.38	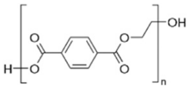
PVC	Isolating cable	Transparent	NUF	0.5 – 1 mm	1.38	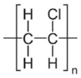

UF: uniform fragment, NUF: non-uniform fragment, NUFF: non-uniform film fragment.

Shapiro-Wilk and Levene's tests, respectively. Although the Shapiro-Wilk test is typically used for larger datasets, we could not perform the more typical Kolmogorov-Smirnov test due to the factor variables involved. For normally distributed and homoscedastic data, a one-way ANOVA, and post-hoc Tukey test where necessary, were applied to complete pairwise analysis of means. Where data were determined to be either not from a normally distributed sample or heteroscedastic, a non-parametric alternative was performed (Kruskal-Wallis and a post-hoc Dunn's test, where necessary). In all cases, a significance level of 0.05 was applied. When means are expressed, deviations (±) are given as standard error.

3. Results

Changes in the physical appearance of the large MiPs were uncommon. However, nylon underwent bleaching when a $ZnCl_2$ density separation solution was used (Figure S3). Upon microscopic examination (method B and method C3), the surface of the large PBAT/PLA particles appeared altered, exhibiting signs of thinning. Furthermore, PP and PS resulted in diminished recoveries when subjected to method C3, possibly due to fragmentation.

3.1. Recovery of large MiPs

The mean recovery of large MiPs across all soils was highest for method B - Fluorescence microscopy (88 ± 4 %), and method A - Digital microscopy (86 ± 3 %), followed by method C1 - ATR-FTIR (80 ± 3 %), and method C3 – µ-Raman (60 ± 17 %) (Table 3). The reduced recoveries observed with the latter method were primarily attributed to MiP analyses of soils with heavier textures, loamy, and clayey (Table 3). For large MiPs only the number of particles rather than their total concentration or mass are routinely determined. Hence, we did not apply ^{1}H NMR and Pyr-GC-MS to large MiPs but exclusively applied these quantification techniques to small MiPs, calculating recoveries based on their absolute content.

Method A - Digital microscopy revealed recovery rates of 80–103 % in sandy soil, 75–105 % in loamy soil, and 75–83 % in clayey soil. These findings suggest that the recoveries remained consistent across different soil textures (Figure S5) and were confirmed by a one-way ANOVA ($p > 0.05$). High recovery rates were accomplished by the introduction of a second decanting step, which significantly enhanced the recovery, resulting in the retrieval of an additional one-third of all plastics (see Supplementary Materials for details). Also, method B - Fluorescence microscopy stood out as highly effective in isolating and identifying large MiPs regardless of the soil type (Table 3 and Figure S5A, B). While this method does not offer precise identification of plastic types, the fluorescence of stained MiP particles varies depending on their characteristics (polarity, morphology, presence of additives, etc.) (Fig. 2). PET and HDPE displayed weaker fluorescence than LDPE and PVC (Fig. 2), occasionally complicating the detection of these MiP particles in spiked soils (Phan Le et al., 2023).

The average recovery for the large MiPs using method C1 - ATR-FTIR ranged from 68 % to 90 % for the different soils, with a better recovery for the finer textured background (Table 3). However, no significant difference between the soil types was observed. We collected up to three spectra of each spiked plastic (0.5 – 1 mm size), which was then added to a reference library (SM Figure S6). Compared with the other methods, method C3 - µ-Raman, faced challenges to identify large MiPs in all three soils (see Supplementary Materials, Figure S5B). We started by applying autofocus settings when obtaining the spectra from the particles on the filters. However, due to much lower recoveries in comparison with the previously mentioned methods, we also applied manual focus for the large particles on the filters MiPs, which led to increased recoveries (Table 3). The recoveries for all three replicates were highest for the

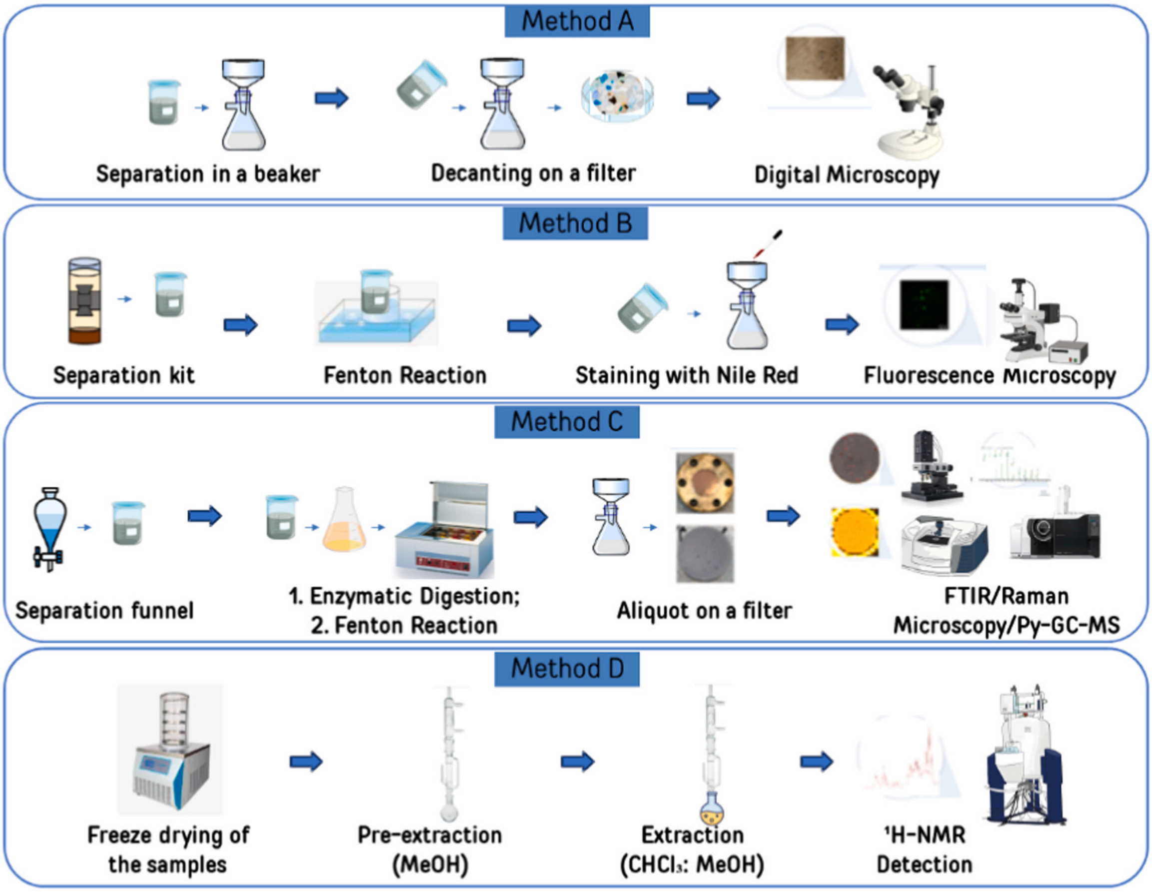

Fig. 1. Illustration of main approaches used for microplastic extraction (SOM = soil organic matter; for additional information on the methods, see also Table S3, Supplementary Materials). For creating the image we used www.bioicons.com, www.flaticons.com and personal library.

Table 3
Mean recoveries (%) with standard error (SE) of large MiPs (0.5–1 mm) for all types of soils; all using microscopical techniques.

	Method A - Digital*			Method B - Fluorescence*			Method C1 - ATR-FTIR			Method C3 - µ-Raman**					
Recoveries	Sandy	Loamy	Clayey	Sandy	Loamy	Clayey	Sandy	Loamy	Clayey	Sandy		Loamy		Clayey	
PP	-	-	-	-	-	-	50 ± 21	60 ± 14	50 ± 7	47 ± 14	53 ± 14	27 ± 5	27 ± 5	40 ± 9	40 ± 16
LDPE	-	-	-	-	-	-	90 ± 7	80 ± 14	80 ± 0	20 ± 0	86 ± 24	20 ± 16	47 ± 24	40 ± 16	73 ± 36
HDPE	-	-	-	-	-	-	70 ± 7	70 ± 7	80 ± 14	127 ± 30	100 ± 41	47 ± 20	47 ± 5	113 ± 14	53 ± 20
PS	-	-	-	-	-	-	60 ± 0	80 ± 28	80 ± 14	13 ± 5	60 ± 9	20 ± 9	60 ± 16	0 ± 0	33 ± 11
PBAT/PLA	-	-	-	-	-	-	80 ± 14	110 ± 7	100 ± 0	140 ± 25	86 ± 5	0 ± 0	40 ± 9	27 ± 22	7 ± 5
PA	-	-	-	-	-	-	90 ± 7	100 ± 0	100 ± 0	73 ± 5	80 ± 9	40 ± 25	47 ± 20	33 ± 14	60 ± 0
PET	-	-	-	-	-	-	90 ± 7	60 ± 14	90 ± 7	87 ± 5	80 ± 9	53 ± 20	13 ± 11	47 ± 20	67 ± 14
PVC	-	-	-	-	-	-	60 ± 0	110 ± 7	90 ± 7	80 ± 9	106 ± 5	40 ± 0	67 ± 5	33 ± 14	73 ± 14
Total	93 ± 5	88 ± 11	79 ± 3	80 ± 4	97 ± 4	89 ± 3	74 ± 4	84 ± 4	84 ± 3	73 ± 10	84 ± 5	31 ± 3	45 ± 3	42 ±10	51 ± 8

[*] No material identification can be performed for large MiPs using digital microscopy and fluorescence staining, since methods are not polymer specific.
[**] Recoveries for µ-Raman microscopy analyses in the first column for each soil are recorded using autofocus, whereas in the second column - applying the focus manually.

sandy soil (73–93 %), followed by the loamy (40–50 %) and the clayey soil (33–63 %), with significant differences between all soil types, shown by an ANOVA and post-hoc Tukey test ($p < 0.05$). As Raman led to a frequent misidentification of PBAT/ PLA as PET, those misidentifications were included in the overall recoveries for PBAT/ PLA. Moreover, PBAT/ PLA spectra showed high noise resulting in poor identification, as already noted by Araujo et al. (2018). For less than 2 % of the cases, PBAT/ PLA was not misidentified as PET but also as PVC, HDPE, and LDPE.

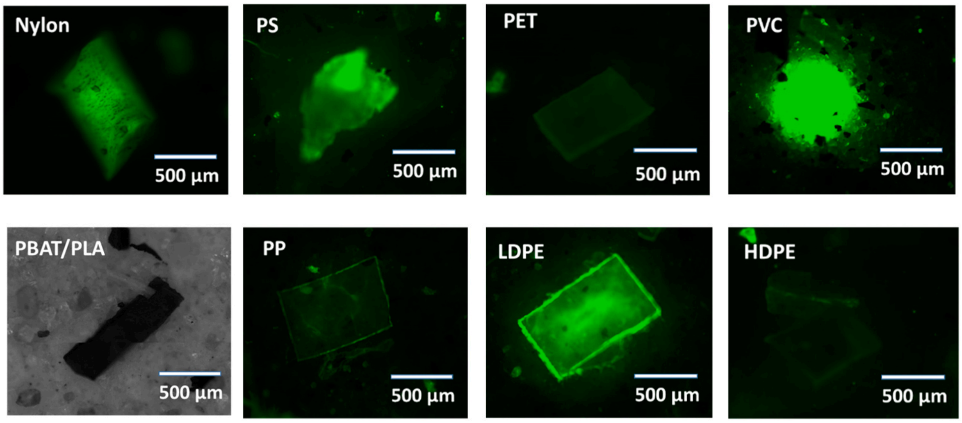

Fig. 2. Fluorescence images of the eight types of different plastic types after their extraction from soil with the described protocol using Nile red staining.

3.2. Recovery of small MiPs

The average recoveries for small MiPs across all soil types varied among the different methods (Figure S7A, B). For LDPE, the highest mean recoveries across the three soil types were achieved with method B – Fluorescence microscopy (62 ± 22 %), followed by method C2 – FPA-µ-FTIR (40 ± 7 %), method C3 - µ-Raman (38 ± 10 %), and method C4 – Pyr-GC-MS (34 ± 5 %), although there were no significant differences between the four ($p > 0.05$). For both PBAT and PLA, method D – ^{1}H NMR yielded the highest recoveries (92 ± 0 % for PBAT and 98 ± 2 % for PLA), followed by method C4 – Pyr-GC-MS (49 ± 21 %), which, however, detects PBAT only while did not find reliable marker signals for PLA in the samples, likely reflecting the very low concentration of the PLA polymer in the biodegradable plastic mulch blend (See Supplementary Materials). Recoveries further tended to decline in the order of method C3 - µ-Raman (39 ± 13 %), method C2 – FPA-µ-FTIR (34 ± 13 %), and method B – Fluorescence (25 ± 15 %) (refer to Fig. 3 for details). Significant differences between the microscopic methods were not observed based on the Kruskal-Wallis test; however, recovery in sandy and loamy soils was significantly higher than in clayey soil ($p < 0.05$) with post-hoc Dunns analysis. It is noteworthy, that ^{1}H NMR provided additional information on the PLA and PBAT content; hence, both components in the biodegradable mulch film were displayed separately in Fig. 3. Across all the microscopic methods, recoveries were consistently higher for conventional LDPE than for biodegradable PBAT/ PLA, except for method D – ^{1}H NMR, as it was tested exclusively for PBAT/ PLA.

For the calculation of particle numbers in spiked soil, the particles found in the non-spiked background and blanks were subtracted (Supplementary Materials, Table S1). Overall, these numbers accounted for 23–98 % of the spiked MiP amounts. For method B – Fluorescence microscopy about 12,500 ± 2400 small LDPE particles were recovered from sandy soil, 13300 ± 1000 from the loamy soil, but only 3800 ± 18,00 from the clayey soil. Considering the expected number of LDPE particles (15,300 ± 4500), and 540–3590 particles in the non-spiked, background soils, this method reached final recoveries for the LDPE of 83–88 % for sandy and loamy soil, but only 8 ± 3 % for the clayey one. For PBAT/ PLA, recovery rates across different soils were notably lower, ranging from 61 ± 3 % in the loamy soil to 5 ± 1 % in the clayey one (Fig. 3). The reduced recovery reflects difficulties in identifying black particles in bright field mode, given that these black PBAT/ PLA particles did not exhibit a distinct fluorescence response to NR staining.

The recoveries of added particles for the small LDPE MiPs for method C2 – FPA-µ-FTIR ranged from 29 ± 0 % for the loamy soil to 57 ± 13 % for the sandy soil. In method C3 - µ-Raman, the recoveries ranged from 13 ± 11 % for clay to 52 ± 4 % for the loamy soil of spiked small MiPs. These were comparatively lower than the recoveries from method B – Fluorescence microscopy, where the overall recovery in sandy and loamy soil was significantly higher than in the clayey one ($p < 0.05$). In contrast, recovery of PBAT/ PLA was similar, ranging from 2 ± 1 % to 50±2 % for the different soils using method C2 – FPA-µ-FTIR, and from 8 ± 6 % to 58 ± 12 % using method C3 - µ-Raman, respectively (Fig. 3). Method C3 - µ-Raman produced more variable outcomes across different soil types than method C2 – FPA-µ-FTIR for small MiPs. A similar pattern was observed for large MiPs. Noteworthy, the identification of PBAT/ PLA was easier when using method C3 - µ-Raman than with method C2 – FPA-µ-FTIR. In all cases, recovering small MiPs was more challenging from the clayey soils than from the sandy ones (Fig. 3). The standard errors of the recoveries for the standard LUFA-loamy soil were much lower than for the other two soils, making the certified soils superior to non-standard environmental soils for such methodological tests. In summary, using FPA-µ-FTIR and µ-Raman techniques holds significant promise for even smaller MiP identification, however, the overall recovery rates across different soil types were not yet satisfactory when utilizing the extraction protocol included in Method C.

As the aliquot used for method C4 – Pyr-GC-MS analysis was obtained from the same final extraction suspension employed for methods C2 – FPA-µ-FTIR and C3 - µ-Raman, this enabled direct comparisons between samples, although it is relevant to acknowledge the presence of a residual mineral fraction in the suspension. The concentrations for LDPE found ranged from 73 to 139 µg g^{-1} (25 ± 4 % to 46 ± 9 % recovery), and for PBAT from 12.5 to 283 µg g^{-1} (4 ± 3 % and 94 ± 17 %) for the different soils, again with the highest recoveries for the sandy soil (Fig. 3).

Finally, method D – ^{1}H NMR provided the most efficient and reliable protocol for the mass determination of biodegradable PBAT/ PLA particles, with recoveries reaching 91–92 % for PBAT and 92–100 % for PLA for the different soils, with standard errors not exceeding 4.1 % in all approaches (Fig. 3).

4. Discussion

When analyzing MiPs, it's noteworthy that while the use of Digital microscopy and staining with fluorescence dye is relatively simple, FPA-µ-FTIR and µ-Raman microscopes are time-consuming with several hours samples processing time, and typically require knowhow and some experience and training even though protocols for their use in analyzing MiPs are somehow well established. Data interpretation is also feasible once a library is used for recognition and a satisfactory matching index is recognized. Pyr-GC-MS in contrast requires more careful data interpretation even though it is one of the most widely used techniques for mass determination of plastics (Steinmetz et al., 2020; Ivleva, 2021). Hence, the joint application of complementary techniques may be needed to give accurate estimates of MiP amounts, particles numbers and size – the latter requires the use of microspectroscopy, despite all challenges (Primpke et al., 2020a,2020b).

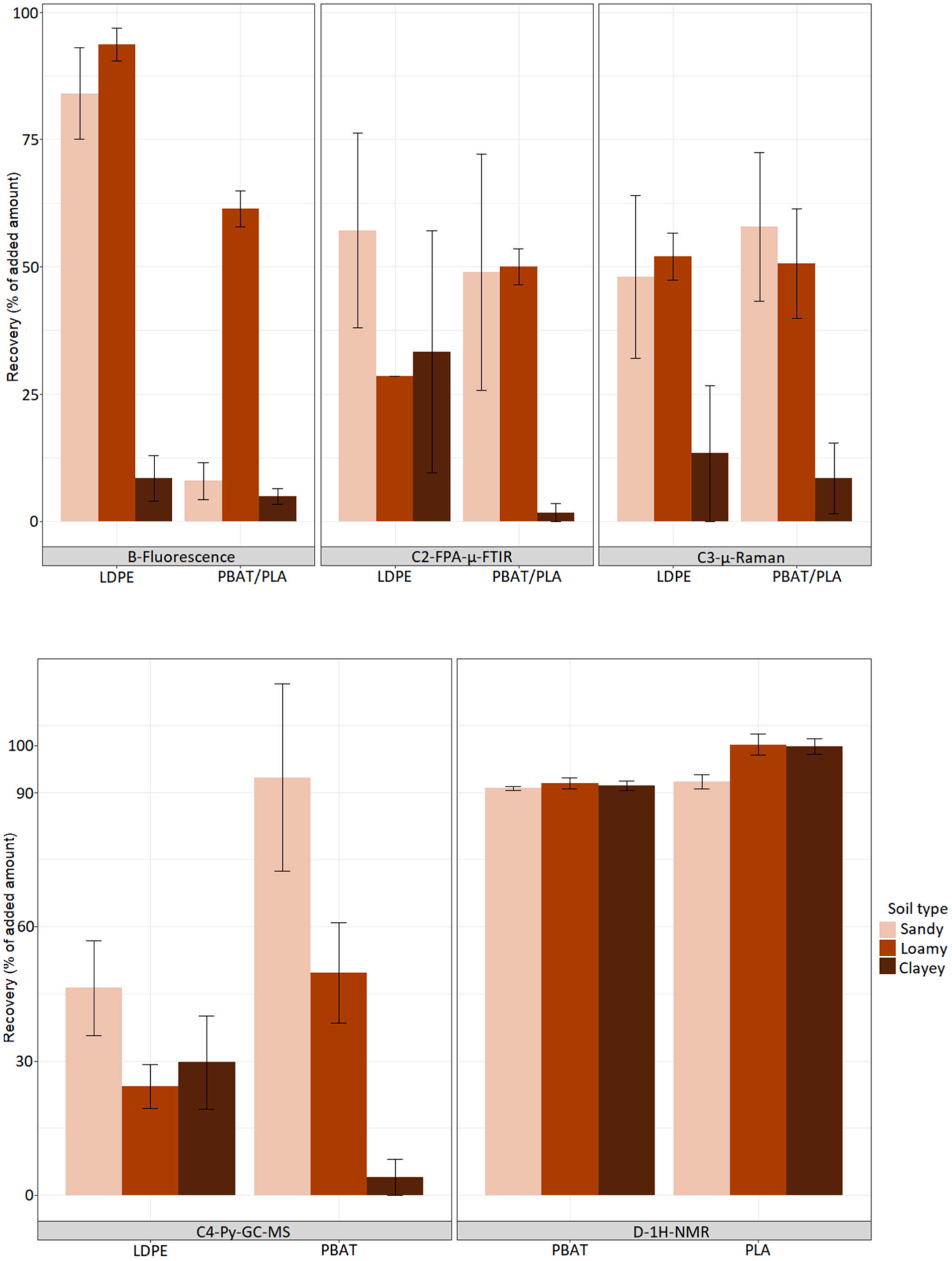

Fig. 3. Recoveries in percent of added amount of particles on the y-axis, of small particles, for LDPE and PBAT/ PLA with methods using particle counting (Figure above), i.e., method B – Fluorescence microscopy, method C2 – FPA-μ-FTIR and method C3 - μ-Raman microscopy and methods assessing bulk polymer amounts, i.e., method C4 - Pyr-GC-MS and method D - ^{1}H NMR (Figure below). Note that ^{1}H NMR allowed a differentiation of PBAT and PLA from the added Mulch-derived MiPs; hence, both polymers are displayed separately. The solvent used for the Soxhlet-extraction was chosen exclusively for PBAT/PLA and Pyr-GC-MS failed to identify PLA. Error bars represent standard errors.

4.1. MiP properties as affected by the extraction method

For plastic extraction from soils and sediments, $ZnCl_2$ is one of the most common salts used for density separation, especially when high-density plastics are analyzed (Coppock et al., 2017; Möller et al., 2020; Prosenc et al., 2021). However, former studies indicate that "harsh" extraction methods may lead to (surface) alteration and fragmentation of MiPs (Hurley et al., 2018; Pfohl et al., 2021). We also observed these alterations in all used protocols for nylon, caused by the corrosive action of $ZnCl_2$ used for density fractionation (Figure S3). As $ZnCl_2$ can act as a Lewis acid due to its hydrolytic activity by generating HCl, $ZnCl_2$ can promote an acidic environment. While Nylon bleaching, the loss of its color, occurred, it did not impact its recovery, nor did it affect the recovery of the other conventional large MiPs (Schrank et al., 2022). However, it is noteworthy, that as nylon is an amide, it can undergo hydrolysis under acidic conditions, which might affect the particles size and for smaller particles presumably even the recovery (Brette et al., 2024).

In contrast, fragmentation with a potential breakdown of large to small MiPs was observed for the PBAT/PLA, as also previously reported by Möller et al. (2021) for biodegradable PLA particles. These alterations may affect both the particle size as well as the spectra of the biodegradable plastics, one potential reason for comparably low recoveries obtained by spectroscopic analyses coupled to microscopical identification, such as in method C. As the spectra of PBAT/PLA particles were only marginally affected by extraction (Figure S9), mainly fragmentation might have caused low recoveries. Consequently, to reduce the potential degradation of biodegradable and conventional plastics during density separation, a replacement of $ZnCl_2$ by other salt solutions, such as the environmentally friendly KCOOH might be suitable (Jarosz et al., 2022).

We explain the low recoveries for PP and PS (leading to a loss of particles that were finally not detected) as well as recoveries that exceed 100 % for PVC (leading to smaller items that were then also counted) with such a fragmentation process. They were presumably caused by mechanical abrasion during the final sieving step from the extraction protocol in method C (Löder et al., 2015; Dong et al., 2020). For the other plastic materials, no secondary MiPs were formed during extraction. We suggest that when digesting SOM with Fenton's reagent and especially when dealing with biodegradable plastics and enzymes like protease (Möller et al., 2021), meticulous attention should be given to these potential fragmentation effects. Conversely, when seeking to characterize surface alterations of plastic particles, as in assessments of plastic weathering in the environment, it might be advisable to refrain from using corrosive substances like $ZnCl_2$ and oxidative chemicals, particularly when subsequent surface-sensitive techniques are used such as Scanning Electron Microscopy. When analyzing biodegradable plastics, Soxhlet extraction combined with ^{1}H NMR stood out compared to other protocols when assessing the total mass of remaining PBAT or PLA.

4.2. Implications for the extraction of large MiPs

All tested methods in this study are frequently described in the literature for MiP analysis (Blasing and Amelung, 2018; Mariano et al., 2021; Wrigley et al., 2024). All methods but method C3 – µ-Raman, yielded recoveries > 75 %. Therefore, we conclude that in principle all are suitable for analyzing large MiPs in soils, enabling comparable results for large MiPs are comparable.

Even the simplest extraction and detection method in method A – Digital microscopy, which only included one density separation and no SOM digestion, recovered between 88 – 93 % of particles across all soils, thus performing at least as reliably as other methods with more sophisticated sample preparation (Braun et al., 2021, 2023). In our tests, the second decanting step after density separation improved recovery substantially and is recommended for further studies. One notable drawback of this method is the inability to identify the type of plastic. This limitation includes the risk of annotating other foreign particles as false positives as MiPs or falsely annotating MiP as SOM, thus introducing errors in the assessment of the number of larger MiP in environmental samples, especially if inexperienced users mistake MiP for SOM, as reported in the case of PBAT/ PLA and black carbon by Mariano et al. (2021). Besides, very small MiP particles can be missed during detection; i.e., as with all other methods, only certain size ranges are reliably analyzed, i.e. with the lowest size limit of 200 µm, as underlined by Kotar et al. (2022).

In summary, the success of Digital microscopy to identify MiP depends on plastic color and size. Hence, the method is problematic when analyzing organic soils due to uncertainties in particle identification (Primpke et al., 2020a,2020b). For other soils, this is less of an issue, and because only images are taken, the methodology does not discriminate against certain plastic materials during detection. We recommend this technique as a fast and simple method for analysis of large MiPs in soil, as no complex pre-treatment besides density fractionation is needed, and many laboratories have access to such microscopes. The analyses of smaller and dark-colored MiPs may demand special training of the operator and/or automatic plastic identification via machine learning (Primpke et al., 2020a,2020b).

Elevated clay and thus usually also elevated SOM contents may not only interfere with detection by introducing interfering compounds on the filters but may also interfere with extraction protocols. Likely, such challenges contributed to generally lower recoveries from the clayey soil, which also contained the highest SOM content. The SOM and clay particles may adhere to MiP, thus potentially forming aggregates that reduce recovery during the density fractionation step, potentially leading to an underestimation of the total MiP content.

A very reliable method for plastic detection other than digital microscopy was the NR staining and particle counting using Fluorescence microscopy in method B (Primpke et al., 2020a,2020b). Recovery rates exceeded 87 %, despite single plastic types showing different staining intensities. Hence, this method is suitable for reliable detection of large MiPs in mineral soils. The result refers to both the efficiency of the NR staining method (except for HDPEs, where the low recoveries occurred due to their dimmed fluorescence with NR) and the extraction efficiency towards larger MiPs (Fig. 2, Figure S8). Using a green fluorescent protein filter set (excitation/emission 470/525 nm) in this study was a valid approach to acquiring fluorescence signals of all plastics (Primpke et al., 2020a,2020b). This is in accordance with previous studies, where green fluorescence was chosen over the red counterpart due to the better fluorescence of synthetic polymers, less fluorescent interference from natural organic matter, and lower background signal intensity in green compared to red fluorescence mode (Shim et al., 2016; Erni-Cassola et al., 2017). Organic digestion with Fenton's reagent did not affect the overall quantitative analysis, even though bleaching of dye/ additive and surface damages were observed. While the extraction process for Fluorescence microscopy takes longer due to the additional Fenton digestion step, data evaluation is faster compared to digital microscopy. This is because Fluorescence microscopy benefits from the automatic quantification of fluorescence-tagged particles through digital image analysis approaches. However, ensuring accuracy and avoiding false-positive identifications still requires expert knowledge. This enables high sample throughput, rendering this method a noteworthy candidate for large environmental monitoring programs. However, the use of automatic quantification with digital image analysis is less reliable and requires additional adjustments when fluorescence intensity varies greatly among different plastics, thus including the risk of overlooking weakly fluorescence MiPs and overestimation of strong fluorescence in SOM, i.e., the analytical result might be more selective to certain plastic types.

The ATR-FTIR and µ-Raman spectroscopies included in method C entail the most sophisticated and time-consuming extraction and purification procedures, along with subsequent detection and data evaluation. In method C the combination of the chosen extraction protocol with subsequent MiP identification using ATR-FTIR and especially μ-Raman spectroscopy yielded lower recoveries than the simpler extractions of one or two steps, which were then followed by the detection via Digital microscopy and Fluorescence microscopy in methods A and B (Table 2). When characterizing with ATR-FTIR in method C1 – ATR-FTIR some large MiPs might have been lost when transferring the particles from the Petri dishes to the sampling stage due to static forces causing the particles to "jump" which has also been observed by Möller et al. (2021) and described in a comprehensible review paper by Primpke et al., (2020a),(2020b). While Löder et al. (2017) documented comparable recoveries for ATR-FTIR, they employed a distinct, more rigorous extraction procedure for PE beads ranging from 180 to 212 μm, whereas our methodology is tailored for larger sizes ranging from 500 to 1000 μm.

Additional challenges were faced during the ATR-FTIR analysis. The enzymatic and oxidative steps needed to reliably recover most plastics generally include the risk of altering the plastic composition, particularly evident in our case for PS and PBAT/PLA, which had matching scores of about 60 % (Radford et al., 2021). As no significant changes were observed in the spectra, we assume alterations of PS were purely physical and that the fragile physical characteristic of the foamy particles resulted in potential shrinkage, thus hindering good contact between the ATR crystal and the surface of the plastic (Prata et al., 2021a, 2021a). For the PBAT/ PLA blend, surface alterations and its black color led to higher absorbance of the IR light (Ribeiro-Claro et al., 2017), which presumably hindered a good matching score. The main difference we noticed between the spectra of the extracted PBAT/ PLA and pristine PBAT/ PLA is expressed as a loss of intensity and broadening of the peaks. Additionally, a slight increase in the shoulder of the peak around 2918 cm^{-1} (-CH_3 stretching) and 2845 cm^{-1} (-CH_2 stretching) was observed, while the two peaks at around 1408 and 1388 cm^{-1} (O-CH_2 bending) almost disappeared for the extracted polymer, presumably due to partial de-esterification in the PBAT (Cai et al., 2013; Figure S9). For PET, PA, HDPE, LDPE, PVC, and PP a matching score > 90 % was accomplished, indicating no changes in the functional groups on the surface of these plastics. Interestingly, for PP lower recoveries were obtained, an explanation for which could be that it was easy to overlook or miss due to its transparency. Overall, we can confirm that ATR-FTIR is a suitable technique for analyzing biodegradable and conventional large MiPs. As the analytical procedure is more time-consuming compared to digital microscopy or fluorescence microscopy, ATR-FTIR is mainly recommended to identify the plastic type. In that case, ATR-FTIR stands out as the main method for identifying the type of meso- or macroplastics.

In method C3 - μ-Raman, PBAT/ PLA required lower laser power than conventional plastic to avoid damage and burning its surface (Ribeiro-Claro et al., 2017). After automatic spectra collection, we observed that most of the spectra were still very noisy. Hence, a manual spectra collection was needed (Table 2). Due to the broad focus range used in automatic recognition, the machine took much longer to identify MiP particles compared to optimized manual settings. To capture the entire filter, approximately 40 minutes were required, and then, depending on the number of identified particles, additional 20–60 minutes are needed for full identification. In manual identification, we adjusted settings for each particle individually to obtain a high-quality spectrum, rather than pre-setting a range for automatic recognition. There are multiple reasons for noise in the spectra of the automatic spectra collection, including: i) the remnants of SOM on the filter, ii) a lack of universally appropriate laser settings for all plastic and the use of a short acquisition time for rapid measurements, iii) the physical necessity of using a 10x objective, iv) surface differences between conventional and biodegradable plastic, v) the possibility that the automatically selected central position of each plastic particle, differs to the bulk of said particle (Araujo et al., 2018; Prata et al., 2021a,2021a). These challenges lead to increases in the signal-to-noise ratios in the spectra as well as the need for stronger laser power to compensate for the lower magnification (Araujo et al., 2018). Unfortunately, due to physical limitations, i.e., the working distance between the filter and the objective itself, it is unfeasible to use objectives with a higher magnification, like 50x or 100x, when analyzing comparable large particles (0.5 – 1 mm).

In summary, method C3 - μ-Raman demonstrated selectivity towards various plastic materials. The weakened resistance of PBAT/ PLA to laser strength, caused by surface degradation due to hydrolysis-prone ester linkages, made the spectra more difficult to detect compared to the virgin PBAT/ PLA blend spectra. Owing to these differences in material resistance, it is thus not feasible to establish a single, specific laser setting (Araujo et al., 2018); additionally, recommended laser energy power ranges from 3 to 4 eV for PBAT/ PLA to 11–12 eV for HDPE. To address inaccuracies resulting from property changes in MiPs, current spectral libraries should be extended to surface-altered plastic types for additional benchmarking or for improving existing references (Dong et al., 2020; Cowger et al., 2021).

In contrast to PBAT/ PLA, MiPs of PET and PVC were very resistant to enzymatic and oxidative steps and showed neat spectra for both automatic and manual recognition. Overall, the Raman spectra changed little, suggesting that functional group composition remained intact for the eight types of conventional plastics. LDPE, in turn, showed strong fluorescence compared with other plastics (Dong et al., 2020; Mariano et al., 2021). A possible explanation could be the presence of additives and that it had black-letter writings on its surface, i.e., the remaining ink may have distorted spectral quality. Overall, Raman thus proved to be efficient for detecting PET, PVC, and PA. The protocol used here, however, was not sufficient to recover the large MiPs from loamy and clayey soils. All in all, Raman still has advantages, particularly in detecting very fine, small MiP items. Nevertheless, it is less recommended for rapid screening of large MiPs in soil.

4.3. Implications for the extraction of small MiPs

In contrast to the large MiPs, the recoveries for the two types of small MiPs (LDPE and the biodegradable PBAT/ PLA) varied. Method B – Fluorescence microscopy was the most efficient in detecting high numbers of small LDPE MiPs, at least for the non-clayey soils. Differences in the recovery of LDPE particles between methods B and C could be due to the number of sample preparation steps, which are fewer for method B – Fluorescence microscopy, or due to the quantity of sample scanned on the filters: for fluorescence microscopy the whole sample extracts (after Fenton digestion) are usually examined, resulting in 2–3 filters per sample, whereas for method C, only 1.5 % v/v of the total extracted sample was analyzed, with higher respective risks that non-representative aliquots are processed. Considering the number of spiked soil sample replicates used, it's worth noting that although triplicates are common in many studies, as emphasized by Ramage et al. (2022), they may not provide sufficient statistical power for robust outcomes. Therefore, running a larger number of replicates is advisable.

For method B – Fluorescence, the fluorescent particles identified in non-spiked soils encompass both "naturally occurring MiPs" and co-stained soil organic residues, especially within the size range of 20–60 μm (see Supplementary Materials, Figure S10). This presence could pose a challenge in the analysis of smaller MiPs (e.g., LDPE $\leq$ 150 μm), leading to false positives, a concern also noted by other authors (e.g., Prata et al., 2021a,2021a). When applying green light at 470 nm, both nonpolar LDPE and these organic parties have strong fluorescent effects (Prata et al., 2019); for other excitation wavelengths, e.g., 560 and 630 nm, interference from fluorescent SOM is expected to be even stronger (Sturm et al., 2021). As a result, background assessment is important when using fluorescence techniques, and background subtraction is needed when establishing the recovery method. Overall, the use of a small MiP isolation (SMI) unit, proposed by Coppock et al. (2017), and the chosen fluorescent microscope settings proved to be a good method for extracting and identifying LDPE particles from soils with low SOM content. Black materials did not fluoresce. Therefore, they interfere with detecting black PBAT/ PLA but not with LDPE.

Unlike LDPE, the recovery rates for PBAT/ PLA MiPs were consistent across the protocols. However, in method C, the recovery rates did not exceed 60 %, indicating potential PBAT/ PLA degradation, low matching indexes, and matrix interferences. These issues were less pronounced in the SOM-poor sandy soils. Consequently, the better extraction for PBAT/ PLA MiPs in this sandy soil using μ-Raman spectroscopy indicated a greater degree of certainty in identifying these black particles on the filter (Fig. 3). The entrapment of particles within clay minerals, particularly when the texture becomes adhesive upon wetting, likely contributed to the loss of these particles for analysis (Primpke et al., 2020a,2020b). It is pivotal, however, to state that μ-FTIR with microscope magnification of 15x is expected to achieve higher recovery rates of the small MiPs since it would be testing pixel sizes of 5.5 μm instead of 20.6 μm. Nevertheless, the processing is more time-consuming and may be cost-prohibitive.

The presence of organic residues affects the smallest size detectable with Raman spectroscopy. In this context, we set a limit of 40 μm due to the presence of noisy spectra for many smaller than 40 μm particles. However, it's worth noting that under different conditions, the limit of detection for Raman spectroscopy can be improved to as low as 1.3 μm, as extensively reviewed by Anger et al. (2018). After conducting the μ-FTIR and μ-Raman analyses, we found no alterations in the spectra of LDPE following the extraction protocol outlined in method C. Thus, for LDPE not surface changes but the increased complexity of steps in this method and potential particle loss may lead to reduced recoveries of small LDPE particles. For PBAT/PLA, additionally surface changes (as observed for FTIR spectra, Figure S9) and fragmentation to sizes below the detection limits of the technique can hamper detection of small MiPs. Hence, there is a need to establish optimized software settings and extraction protocol steps (Primpke et al., 2020a,2020b). The advantage of using $ZnCl_2$ as heavy density liquid is then hampered by the corrosive nature of the reagent for these materials. Additionally, comprehensive investigations into structural changes in particles, especially as their surface-to-volume ratio increases, are imperative.

Method C4 - Pyr-GC-MS, similar to methods C2 – FPA-μ-FTIR and C3 - μ-Raman, necessitated subsampling of an aliquot before analysis due to the inability to assess the entire extracted solution. Despite this, we achieved a recovery of 94 % (± 17 %) for PBAT in sandy soil, suggesting that subsampling for the total mass analyses of MiP is not a problem per se. Difficulties to recover LDPE-MiP and other PBAT particles in loamy and clayey soil (Fig. 3) are thus likely related to some SOM and soil minerals still being present (Figure S11; Primpke et al., 2020a,2020b; Cheng et al., 2021; Bouzid et al., 2022). These minerals can affect pyrolysis yields and may adsorb pyrolysis products of the polymers before they are transmitted to the mass spectrometer (Bouzid et al., 2022). To better control samples' heterogeneity, Steinmetz et al. (2020) adopted a dissolving approach using 1, 2, 4 – trichlorobenzene to analyze PP, PE and PS in soil samples via Pyr-GC-MS without any further treatment. However, this method excludes polymers like PET that do not dissolve in this solvent and requires further optimization for better matrix cleanup.

On the other hand, dissolving polymers in suitable solvents and afterwards quantifying via ^{1}H NMR spectroscopy analysis offers a fast and high-throughput extraction technique particularly for biodegradable plastics. Using chloroform: methanol – 9:1 as a solvent for the PBAT/ PLA mulch film extraction in method D – ^{1}H NMR proved to be exceptionally efficient for extracting and further analyzing these biodegradable MiPs. Additionally, ^{1}H NMR has demonstrated its effectiveness as a method for quantifying a wide range of polymers, including LDPE, PET, PS, PVC, ABS, PA, and PBAT, within diverse and complex matrices (Ivleva et al., 2021).

In general, for smaller MiPs, lower recoveries and larger errors were observed compared to large MiPs. Larger particles are less efficiently absorbed and more effectively separated during density separation (Kotar et al., 2022). On the contrary, this effect is irrelevant for the small-sized MiPs as their larger specific surface area makes them more prone to being lost through adsorption (Primpke et al., 2020a,2020b). Therefore, if there is no need to determine the number and size of MiP particles but rather the total amount, we recommend employing method D – Soxhlet - extraction coupled with ^{1}H NMR spectroscopy.

5. Conclusions

Comparing different methodologies for the extraction and detection of large MiPs (0.5–1 mm) showed that their analyses are reliable for samples extracted from soils, a pattern likely perceived for other environmental samples. Digital microscopy already performed well in screening MiPs without excessive sample pretreatment, i.e., this respective method protocol is useful for fast comparisons of larger sampling sets. Yet, staining of the particles followed by Fluorescence microscopy stood out in terms of short protocol duration and reliability. Additional detection techniques such as ATR-FTIR or μ-Raman spectroscopy are, however, necessary for the identification of the MiP type. While μ-FTIR and μ-Raman spectroscopy can potentially identify very small MiPs, it is more sensitive to sample inhomogeneity when smaller volumes are used and can be affected by organic residues, resulting in an approximate loss of roughly 50 % of particles in our case. This low recovery rate is a critical concern, particularly when MiP analyses are intended for legislative monitoring. Future efforts to quantify and compensate for these losses, such as the use of appropriate surrogate standards, require immediate attention. Yet, even though the analyses of small MiPs are more challenging, excellent recoveries were recorded with Fluorescence microscopy for small LDPE MiPs (sandy and loamy soil), and the biodegradable PBAT/ PLA blends using Soxhlet - extraction followed by quantitative ^{1}H NMR.

CRediT authorship contribution statement

Stoyana Tsvetanova Peneva: Writing – original draft, Visualization, Validation, Methodology, Investigation, Formal analysis, Data curation. **Quynh Nhu Phan Le:** Writing – review & editing, Visualization, Validation, Methodology, Investigation, Data curation. **Davi Munhoz:** Writing – review & editing, Visualization, Validation, Methodology, Investigation, Data curation. **Olivia Wrigley:** Writing – review & editing, Visualization, Methodology, Investigation. **Flora Wille:** Writing – review & editing, Validation, Methodology, Investigation, Data curation. **Heidi Doose:** Writing – review & editing, Visualization, Supervision. **Crispin Halsall:** Writing – review & editing, Visualization, Supervision, Conceptualization. **Paula Harkes:** Writing – review & editing, Supervision. **Michael Sander:** Writing – review & editing, Visualization, Validation, Supervision, Methodology. **Melanie Braun:** Writing – review & editing, Visualization, Supervision, Investigation, Conceptualization. **Wulf Amelung:** Writing – review & editing, Visualization, Supervision, Methodology, Investigation, Conceptualization.

Declaration of Competing Interest

The authors declare that they have no known competing financial interests or personal relationships that could have appeared to influence the work reported in this paper.

Acknowledgements

This work was supported by the European Union's Horizon 2020, ITN SOPLAS, with grant agreement No. 955334 to the five first authors. The authors thank Elisabeth Shaw and Alexandre Benedetto (Lancaster University) for their help with the fluorescence microscope measurement; Markus Rhode, Ulrich Meinke and Sven Simons (Wessling GmbH) for the expertise provided for the measurements with Raman Microscope and Pyrolysis–Gas Chromatography–Mass Spectroscopy; Prof Violette Geissen for supporting and supervising the work done at

Wageningen University and Research.

Appendix A. Supporting information

Supplementary data associated with this article can be found in the online version at doi:10.1016/j.ecoenv.2024.117428.

Data availability

Data will be made available on request.

References

Anger, Pm, von der Esch, E., Baumann, T., Elsner, M., Niessner, R., Ivleva, N.P., 2018. Raman microspectroscopy as a tool for microplastic particle analysis. TrAC Trends Anal. Chem. 109, 214–226. https://doi.org/10.1016/j.trac.2018.10.010.

Araujo, C.F., Nolasco, M.M., Ribeiro, A.M.P., Ribeiro-Claro, P.J.A., 2018. Identification of microplastics using Raman spectroscopy: Latest developments and future prospects. Water Res 142, 426–440. https://doi.org/10.1016/j.watres.2018.05.060.

Astner, A.F., Gillmore, A.B., Yu, Y., Flury, M., DeBruyn, J.M., Schaeffer, S.M., Hayes, D. G., 2023. Formation, behavior, properties and impact of micro- and nanoplastics on agricultural soil ecosystems (A Review). NanoImpact 31, 100474. https://doi.org/10.1016/j.impact.2023.100474.

Bläsing, M., Amelung, W., 2018. Plastics in soil: analytical methods and possible sources. Sci. Total Environ. 612, 422–435. https://doi.org/10.1016/j.scitotenv.2017.08.086.

Bouzid, N., Anquetil, C., Dris, R., Gasperi, J., Tassin, B., Derenne, S., 2022. Quantification of microplastics by pyrolysis coupled with gas chromatography and mass spectrometry in sediments: challenges and implications. Microplastics 1, 229–239. https://doi.org/10.3390/microplastics1020016.

Braun, M., Mail, M., Heyse, R., Amelung, W., 2021. Plastic in compost: prevalence and potential input into agricultural and horticultural soils. Sci. Total Environ. 760, 143335. https://doi.org/10.1016/j.scitotenv.2020.143335. Epub 2020 Nov 4. PMID: 33199003.

Braun, M., Mail, M., Krupp, A.E., Amelung, W., 2023. Microplastic contamination of soil: are input pathways by compost overridden by littering? Sci. Total Environ. 855, 158889. https://doi.org/10.1016/j.scitotenv.2022.158889.

Brette, M.M., Holm, A.H., Drozdov, A.D., Christiansen, Jd.C., 2024. Pure hydrolysis of polyamides: a comparative study. Chemistry 6, 13–50. https://doi.org/10.3390/chemistry6010002.

Büks, F., Kaupenjohann, M., 2020. Global concentrations of microplastics in soils – a review. SOIL 6, 649–662. https://doi.org/10.5194/soil-6-649-2020.

Cai, Y., Lv, J., Feng, J., 2013. Spectral characterization of four kinds of biodegradable plastics: poly (lactic acid), poly (butylenes adipate-co-terephthalate), poly (hydroxybutyrate-co-hydroxyvalerate) and poly (butylenes succinate) with FTIR and Raman spectroscopy. J. Polym. Environ. 21, 108–114. https://doi.org/10.1007/s10924-012-0534-2.

Caputo, F., Vogel, R., Savage, J., Vella, G., Law, A., Della Camera, G., Hannon, G., Peacock, B., Mehn, D., Ponti, J., Geiss, O., Aubert, D., Prina-Mello, A., Calzolai, L., 2021. Measuring particle size distribution and mass concentration of nanoplastics and microplastics: addressing some analytical challenges in the sub-micron size range. J. Colloid Interface Sci. 588, 401–417. https://doi.org/10.1016/j.jcis.2020.12.039.

Cheng, M.L.H., Lippmann, T.C., Dijkstra, J.A., Bradt, G., Cook, S., Choi, J.G., Brown, B.L., 2021. A baseline for microplastic particle occurrence and distribution in Great Bay Estuary. Mar. Pollut. Bull. 170, 112653. https://doi.org/10.1016/j.marpolbul.2021.112653.

Coppock, R.L., Cole, M., Lindeque, P.K., Queirós, A.M., Galloway, T.S., 2017. A small-scale, portable method for extracting microplastics from marine sediments. Environ. Pollut. 230, 829–837. https://doi.org/10.1016/j.envpol.2017.07.017.

Cowger, W., Steinmetz, Z., Gray, A., Munno, K., Lynch, J., Hapich, H., Primpke, S., De Frond, H., Rochman, C., Herodotou, O., 2021. Microplastic spectra classification needs an open source community: open specy to the rescue! Anal. Chem. 93 (21), 7543–7548. https://doi.org/10.1021/acs.analchem.1c00123.

Dong, M., Zhang, Q., Xing, X., et al., 2020. Raman spectra and surface changes of microplastics weathered under natural environments. Sci. Total Environ. 739, 139990. https://doi.org/10.1016/j.scitotenv.2020.139990.

Dümichen, E., Eisentraut, P., Bannick, C.G., Barthel, A.K., Senz, R., Braun, U., 2017. Fast identification of microplastics in complex environmental samples by a thermal degradation method. Chemosphere 174, 572–584. https://doi.org/10.1016/j.chemosphere.2017.02.010.

El Hayany, B., El Fels, L., Quénéa, K., Dignac, M.F., Rumpel, C., Gupta, V.K., Hafidi, M., 2020. Microplastics from lagooning sludge to composts as revealed by fluorescent staining- image analysis, Raman spectroscopy and pyrolysis-GC/MS. J. Environ. Manag. 275, 111249. https://doi.org/10.1016/j.jenvman.2020.111249.

Erni-Cassola, G., Gibson, M.I., Thompson, R.C., Christie-Oleza, J.A., 2017. Lost, but found with Nile red: A rapid and inexpensive technique to detect and quantify small microplastics by fluorescence microscopy. Environ. Sci. Technol. 51 (23), 13641–13648. https://doi.org/10.1021/acs.est.7b04512.

Fox, J., Weisberg, S., 2019. An R Companion to Applied Regression, Third edition. Sage, Thousand Oaks CA. ⟨https://socialsciences.mcmaster.ca/jfox/Books/Companion/⟩.

Han, X., Lu, X., Vogt, R.D., 2019. An optimized density-based approach foe extracting microplastics from soil and sediment samples. Environ. Pollut. https://doi.org/10.1016/j.envpol.2019.113009.

He, D., Luo, Y., Lu, S., Liu, M., Song, Y., Lei, L., 2018. Microplastics in soils: Analytical methods, pollution characteristics and ecological risks. TrAC Trends in Analytical Chemistry 109, 163–172.

Hurley, R.R., Lusher, A.L., Olsen, M., Nizzetto, L., 2018. Validation of a method for extracting microplastics from complex, organic-rich, environmental matrices. Environ. Sci. Technol. 52 (13), 7409–7417. https://doi.org/10.1021/acs.est.8b01517.

Imhof H.K., Schmid J., Niessner R., Ivleva N.P., Laforsch C. 2012. A novel, highly efficient method for separation and quantification of plastic particles in sediments of aquatic environments, p. 524-537 ⟨https://doi.org/10.4319/lom.2012.10.524⟩.

Ivleva, N.P., 2021. Chemical analysis of microplastics and nanoplastics: challenges, advanced methods, and perspectives. Chem. Rev. 121 (19), 11886–11936. https://doi.org/10.1021/acs.chemrev.1c00178.

Jarosz, K., Natkański, P., Michalik, M., 2022. Microplastic extraction from the sediment using potassium formate water solution (H_2O/KCOOH). Minerals 12, 269. https://doi.org/10.3390/min12020269.

Junhao, C., Xining, Z., Xiaodong, G., Li, Z., Qi, H., Siddique, H.M.K., 2021. Extraction and identification methods of microplastics and nanoplastics in agricultural soil: a review. J. Environ. Manag. 294, 112997. https://doi.org/10.1016/j.jenvman.2021.112997.

Kittner, M., Eisentraut, P., Dittmann, D., Braun, U., 2023. Decomposability versus detectability: First validation of TED-GC/MS for microplastic detection in different environmental matrices. Appl. Res. https://doi.org/10.1002/appl.202200089.

Kotar, S., McNeish, R., Murphy-Hagan, C., Renick, V., Lee, C.T., Steele, C., Lusher, A., Moore, C., Minor, E., Schroeder, J., Helm, P., Rickabaugh, K., De Frond, H., Gesulga, K., Lao, W., Munno, K., Thornton Hampton, L.M., Weisberg, S.B., Wong, C. S., Amarpuri, G., Andrews, R.C., Barnett, S.M., Christiansen, S., Cowger, W., Crampond, K., Du, F., Gray, A.B., Hankett, J., Ho, K., Jaeger, J., Lilley, C., Mai, L., Mina, O., Lee, E., Primpke, S., Singh, S., Skovly, J., Slifko, T., Sukumaran, S., van Bavel, B., Van Brocklin, J., Vollnhals, F., Wu, C., Rochman, C.M., 2022. Quantitative assessment of visual microscopy as a tool for microplastic research: recommendations for improving methods and reporting. Chemosphere 308 (Pt 3), 136449. https://doi.org/10.1016/j.chemosphere.2022.136449. Epub 2022 Sep 14. PMID: 36115477.

Lebreton, L., van der Zwet, J., Damsteeg, J.W., et al., 2017. River plastic emissions to the world's oceans. Nat. Commun. 8, 15611. https://doi.org/10.1038/ncomms15611iSQAPER.

Löder, M.G.J., Imhof, H.K., Ladehoff, M., Löschel, L.A., Lorenz, C., Mintenig, S., Piehl, S., Primpke, S., Schrank, I., Laforsch, C., Gerdts, G., 2017. Enzymatic purification of microplastics in environmental samples. Environ. Sci. Technol. 51 (24), 14283–14292. https://doi.org/10.1021/acs.est.7b03055.

Mani, T., Frehland, S., Kalberer, A., Burkhardt-Holm, P., 2019. Using castor oil to separate microplastics from four different environmental matrices. Anal. Methods 11, 1788–1794. https://doi.org/10.1039/C8AY02559B.

Mariano, S., Tacconi, S., Fidaleo, M., Rossi, M., Dini, L., 2021. Micro and nanoplastics identification: classic methods and innovative detection techniques. Front Toxicol. 3, 636640. https://doi.org/10.3389/ftox.2021.636640.

Mbachu, O., Jenkins, G., Pratt, C., Kaparaju, P., 2021. Enzymatic purification of microplastics in soil. MethodsX 8, 101254. https://doi.org/10.1016/j.mex.2021.101254.

Mintenig, S.M., Int-Veen, I., Löder, M.G.J., Primpke, S., Gerdts, G., 2017. Identification of microplastic in effluents of waste water treatment plants using focal plane array-based micro-Fourier-transform infrared imaging. Water Res 108, 365–372. https://doi.org/10.1016/j.watres.2016.11.015.

Möller, J.N., Heisel, I., Satzger, A., Vizsolyi, E.C., Jacob Oster, S.D., Agarwal, S., Laforsch, C., Loder, M.G.J., 2021. Tackling the challenge of extracting microplastics from soils: a protocol to purify soil samples for spectroscopic analysis. Environ. Toxicol. Chem. https://doi.org/10.1002/etc.5024.

Möller, J.N., Loder, M.G.J., Laforsch, C., 2020. Finding microplastics in soil: a review of analytical methods. Environ. Sci. Technol. 54 (4), 2078–2090. https://doi.org/10.1021/acs.est.9b04618.

Nelson, T.F., Remke, S.C., Kohler, H.P.E., McNeill, K., Sander, M., 2019. Quantification of Synthetic Polyesters from Biodegradable Mulch Films in Soils. Environ. Sci. Technol.

Nuelle, M.T., Dekiff, J.H., Remy, D., Fries, E., 2014. A new analytical approach for monitoring microplastics in marine sediments. Environ. Pollut. 184, 161–169. https://doi.org/10.1016/j.envpol.2013.07.027.

OECD Policy Highlights, Global Plastic Outlook Database: Economic Drivers, Environmental Impacts and Policy Opitons, 2022, ⟨https://doi.org/10.1787/de747aef-en⟩,

Ogle D.H., Doll J.C., Wheeler A.P., Dinno A. (2023). FSA: Simple Fisheries Stock Assessment Methods. R package version 0.9.5, ⟨https://CRAN.R-project.org/package=FSA⟩.

Perez, C.N., Carre, F., Hoarau-Belkhiri, A., Joris, A., Leonardis, P.E.G., Lamoree, M.H., 2022. Innovations in analytical methods to assess the occurance of microplastics in soil. J. Environ. Chem. Eng. 10 (3), 107421. https://doi.org/10.1016/j.jece.2022.107421.

Pfohl, P., Roth, C., Meyer, L., et al., 2021. Microplastic extraction protocols can impact the polymer structure. Micro Nanopl 1, 8. https://doi.org/10.1186/s43591-021-00009-9.

Phan Le, Q.N., Halsall, C., Peneva, S., Wridley, O., Amelung, W., Braun, M., Quinton, J., Surridge, B., 2023. Towards quality-assured measurements of microplastics in soils using fluorescence microscopy. EGU Gen. Assem. https://doi.org/10.5194/egusphere-egu23-13873.

PlasticsEurope, 2023. *Plastics - the fast facts 2023*. *https://plasticseurope.org/knowledge-hub/plastics-the-fast-facts-2023/*.

Prata, Joana, Da Costa, Joao, Fernandes, Antonio, Costa, Florinda, Duarte, Armando, Rocha-Santos, Teresa, 2021b. Selection of microplastics by Nile Red staining increases environmental sample throughput by micro-Raman spectroscopy. Sci. Total Environ. 783, 146979. https://doi.org/10.1016/j.scitotenv.2021.146979.

Prata, J.C., Reis, V., Matos, J.T.V., da Costa, Duarte, A.C., Duarte, A.C., Rocha-Santos, T., 2019. A new approach for routine quantification of microplastics using Nile Red and automated software (MP-VAT). Sci. total environ. 690, 1277–1283. https://doi.org/10.1016/j.scitotenv.2019.07.060.

Prata, Joana, Sequeira, Inês, Monteiro, Silvia, Patricio Silva, A.L., Da Costa, Joao, Dias-Pereira, Patrícia, Fernandes, Antonio, Costa, Florinda, Duarte, Armando, Rocha-Santos, Teresa, 2021a. Preparation of biological samples for microplastic identification by Nile Red. Sci. Total Environ. 783, 147065. https://doi.org/10.1016/j.scitotenv.2021.147065.

Primpke, S., Christiansen, S.H., Cowger, W., et al., 2020b. Critical assessment of analytical methods for the harmonized and cost-efficient analysis of microplastics. Appl. Spectrosc. 74 (9), 1012–1047. https://doi.org/10.1177/0003702820921465.

Primpke, S., Fischer, M., Lorenz, C., et al., 2020a. Comparison of pyrolysis gas chromatography/mass spectrometry and hyperspectral FTIR imaging spectroscopy for the analysis of microplastics. Anal. Bioanal. Chem. 412, 8283–8298. https://doi.org/10.1007/s00216-020-02979-w.

Primpke, S., Wirth, M., Lorenz, C., et al., 2018. Reference database design for the automated analysis of microplastic samples based on Fourier transform infrared (FTIR) spectroscopy. Anal. Bioanal. Chem. 410, 5131–5141. https://doi.org/10.1007/s00216-018-1156-x.

Prosenc, F., Leban, P., Šunta, U., Bavcon Kralj, M., 2021. Extraction and identification of a wide range of microplastic polymers in soil and compost. Polymers 13, 4069. https://doi.org/10.3390/polym13234069. ⟨https://plasticseurope.org/knowledge-hub/plastics-the-facts-2022/⟩.

R Core Team (2018). R: A language and environment for statistical computing. R Foundation for Statistical Computing, Vienna, Austria. URL: ⟨https://www.R-project.org/⟩.

Radford, F., Zapata-Restrepo, L.M., Horton, A.A., Hudson, M.D., Shaw, P.J., Williams, I. D., 2021. Developing a systematic method for extraction of microplastics in soils. Anal. Methods. https://doi.org/10.5258/SOTON/D1455.

Ramage, S.J.F.F., Pagaling, E., Haghi, R.K., Dawson, L.A., Yates, K., Prabhu, R., Hillier, S., Devalla, S., 2022. Rapid extraction of high- and low-density microplastics from soil using high-gradient magnetic separation. Sci. Total Environ. 831, 154912. https://doi.org/10.1016/j.scitotenv.2022.154912. Epub 2022 Mar 29. PMID: 35364148.

Ribeiro-Claro, Paulo J.A., et al., 2017. Chapter 5 - characterization of microplastics by Raman Spectroscopy. Compr. Anal. Chem. 75, 119–151.

Sajjad, M., Huang, Q., Kahn, S., Khan, M.A., Liu, Yin, Wang, J., Lian, F., Wang, Q., Guo, G., 2022. Microplastics in the soil environment: a critical review. Environ. Technol. Innov. https://doi.org/10.1016/j.eti.2022.102408.

Schrank, I., Möller, J.N., Imhof, H.K., Hauenstein, O., Zielke, F., Agarwal, S., Löder, M.G. J., Greiner, A., Laforsch, C., 2022. Microplastic sample purification methods - assessing detrimental effects of purification procedures on specific plastic types. Sci. Total Environ. 833, 154824. https://doi.org/10.1016/j.scitotenv.2022.154824.

Shim W.J., Song Y.K., Hong S.H., Jang M. 2016. Identification and quantification of microplastics using Nile Red staining, Marina Pollution Buletin Volume 113, Issues 1–2, 15 December 2016, Pages 469-476 https://doi.org/10.1016/j.marpolbul.2016.10.049.

Steinmetz, Z., Kintzi, A., Munoz, Katherine, Schaumann, G.E., 2020. A simple method for the selective qunatification of polyethylene, polypropylene, and polystyrene plastic debris in soil by pyrolysis-gas chromatography/mass spectrometry. J. Anal. Appl. Pyrolysis 147, 104803. https://doi.org/10.1016/j.jaap.2020.104803.

Sturm, M.T., Horn, H., Schuhen, K., 2021. The potential of fluorescent dyes—comparative study of Nile red and three derivatives for the detection of microplastics. Anal. Bioanal. Chem. 413, 1059–1071. https://doi.org/10.1007/s00216-020-03066-w.

Wang, Y., Xiang, L., Amelung, W., Elsner, M., Gan, J., Kueppers, S., Laforsch, C., Jiang, X., Adu-Gyamfi, J., Heng, Sik Ok, Y., Ivleva, N.P., Luo, Y., Barceló, D., Schäffer, A., Wang, F., 2023. Micro- and nanoplastics in soil ecosystems: analytical methods, fate, and effects. TrAC Trends Anal. Chem., 117309 https://doi.org/10.1016/j.trac.2023.117309.

Way, C., Hudson, M.D., Williams, I.D., Langley, G.J., 2022. Evidence of underestimation in microplastic research: a meta-analysis of recovery rate studies. Sci. Total Environ. 805, 150227. https://doi.org/10.1016/j.scitotenv.2021.150227. Epub 2021 Sep 9. PMID: 34537704.

Wickham, H. ggplot2: Elegant Graphics for Data Analysis. ⟨https://doi.org/10.1007/978-3-319-24277-4⟩.

Wrigley, O., Braun, M., Amelung, W., 2024. Global soil microplastic assessment in different land-use systems is largely determined by the method of analysis: A meta-analysis. Sci. Total Environ. 957, 177226.

Zhang, S., Yang, X., Gertsen, H., Peters, P., Salánki, T., Geissen, V., 2018. A simple method for the extraction and identification of light density microplastics from soil. Sci. Total Environ. 616-617, 1056–1065. https://doi.org/10.1016/j.scitotenv.2017.10.213.

Zhou, B., Wang, J., Zhang, H., Shi, H., Fei, Y., Huang, S., et al., 2020. Microplastics in Agricultural Soils on the Coastal plain of Hangzhou Bay, east China: Multiple Sources Other Than Plastic Mulching Film. J. Hazard. Mater. 388, 121814. https://doi.org/10.1016/j.jhazmat.2019.121814.